(2

CAR-TR-114
CS-TR-1485

DAAK70-83-K-0018
April 1985

ON THE UNIQUENESS OF IMAGE FLOW SOLUTIONS FOR PLANAR SURFACES IN MOTION

Muralidhara Subbarao
Allen M. Waxman

Center for Automation Research
University of Maryland
College Park, MD 20742

COMPUTER VISION LABORATORY

CENTER FOR AUTOMATION RESEARCH

UNIVERSITY OF MARYLAND
COLLEGE PARK, MARYLAND
20742

(2)

(A)

CAR–TR–114
CS–TR–1485

DAAK70–83–K–0018
April 1985

ON THE UNIQUENESS OF IMAGE FLOW SOLUTIONS FOR PLANAR SURFACES IN MOTION

Muralidhara Subbarao
Allen M. Waxman

Center for Automation Research
University of Maryland
College Park, MD 20742

This document has

ABSTRACT

Two important results relating to the uniqueness of image flow solutions for planar surfaces in motion are presented here. These results relate to the formulation of the image flow problem by Waxman and Ullman [1], which is based on a kinematic analysis of the image flow field. The first result concerns resolving the duality of interpretations that are generally associated with the instantaneous image flow of an evolving image sequence. It is shown that the interpretation for orientation and motion of planar surfaces is unique when either two successive image flows of one planar surface patch are given or one image flow of two planar patches moving as a rigid body is given. We have proved this by deriving explicit expressions for the evolving solution of an image flow sequence with time. These expressions can be used to resolve this ambiguity of interpretation in practical problems. The second result is the proof of uniqueness for the velocity of approach which satisfies the image flow equations for planar surfaces derived in ~~[1]~~. In addition, it is shown that this velocity can be computed as the middle root of a cubic equation. These two results together suggest a new method for solving the image flow problem for planar surfaces in motion.

Waxman's and Ullman's document.

image flow equations, additional keywords:

The support of the Defense Advanced Research Projects Agency and the U.S. Army Night Vision Laboratory under Contract DAAK70–83–K–0018 (DARPA Order 3206) is gratefully acknowledged.

1. INTRODUCTION

The relative motion of a pin-hole camera with respect to a rigid, textured surface results in a time-varying image on its projection screen. The image flow problem concerns the recovery of space motion and surface structure by analyzing its evolving image sequence. Waxman and Ullman [1] developed a formulation of the image flow problem in which the motion and structure parameters of the surface are given by the solution of a set of twelve non-linear algebraic equations. These equations were derived by a kinematic analysis of the image flow field. This paper extends this earlier work of Waxman and Ullman for the special case of planar surfaces in motion.

There are two important results presented in this paper which relate to the uniqueness of solutions for planar surfaces in motion. Our first result concerns the uniqueness of interpretation for orientation and motion. Given two successive image frames (or the instantaneous flow) of an image sequence, it has been shown by Waxman and Ullman [1] that there are generally two interpretations which are duals of each other. In this paper we show that this duality can be resolved to give a unique interpretation when either three successive image frames (or two successive flows) of one planar surface patch are given, or two frames (or one flow field) with two planar patches moving as a rigid body are given. A similar result has been obtained from a different approach in the 4-point formulation of Tsai and Huang [3]. Our approach to the first case consists of deriving explicit expressions for the evolving solution over successive image frames for the two dual

interpretations, and then comparing these expressions at a later time when they are no longer dual. These expressions can be used in practical problems to resolve the ambiguity in interpretation. In the second case, we simply note that the spurious solutions for orientations are the same and the rotation parameters are (in general) different for all planar surfaces which are stationary with respect to each other in space. Our second main result concerns the uniqueness of the translational velocity component along the line of sight. Waxman and Ullman's solution of the image flow equations suggested that this velocity was, indeed, uniquely determined (with the duality described above being the sole form of non-uniqueness); however, this was not proved. Here, we show that given only the instantaneous image flow, the velocity component along the line of sight is uniquely determined. Further, it is shown that this velocity component can be computed as the middle root of a cubic equation. These results are derived directly from the formulation of the image flow problem in [1]. Reference to a similar result recently obtained by Longuet-Higgins for a different formulation of the problem is found in Buxton [4].

The organization of this paper is as follows. In the next section we briefly summarize the formulation of the image flow problem of Waxman and Ullman [1] for planar surfaces. In Section 3, we discuss and illustrate the dual nature of planar surface solutions. In Section 4, uniqueness of interpretation for orientation and motion of planar surfaces two image flows is proved. In Section 5, the uniqueness of the translational velocity component along the line of sight for the

instantaneous image flow is proved. Our results in Sections 4 and 5 lead to a new method for solving the structure and motion of a planar surface, which is outlined in Section 6.

2. FORMULATION OF THE IMAGE FLOW PROBLEM

The relationship between a rigid object's structure and motion and the generated image flow field has been discussed by Waxman and Ullman[1]. Their formulation in terms of "observables" or "deformation parameters" [2] is central to the approach taken here.

2.1 Coordinate System and Notation

We attribute the relative rigid body motion to an observer represented by the spatial coordinate system (X, Y, Z) in Figure 1. The origin of this system is located at the vertex of perspective projection, and the Z-axis is directed along the center of the instantaneous field of view. The instantaneous rigid body motion of this coordinate system is specified in terms of the translational velocity $\boldsymbol{V} = (V_X, V_Y, V_Z)$ of its origin and its rotational velocity $\boldsymbol{\Omega} = (\Omega_X, \Omega_Y, \Omega_Z)$. The 2-D image sequence is created by the perspective projection of the object onto a planar screen oriented normal to the Z-axis. The origin of the image coordinate system (x, y) on the screen is located in space at $(X, Y, Z) = (0, 0, 1)$; that is, the image is reinverted and scaled to a focal length of unity.

Due to the observer's motion, a point P in space (located by position vector $\boldsymbol{R}$) moves with a relative velocity $\boldsymbol{U} = -(\boldsymbol{V} + \boldsymbol{\Omega} \times \boldsymbol{R})$. At each instant, point P projects onto the screen as point p with coordinates

$$(x, y) = (X/Z, Y/Z). \tag{1}$$

The corresponding image velocities of point p are $(v_x, v_y) = (\dot{x}, \dot{y})$, obtained

by differentiating the image coordinates with respect to time and utilizing the components of U for the time derivatives of the spatial coordinates of P. The result is

$$v_x = \left\{ x \frac{V_Z}{Z} - \frac{V_X}{Z} \right\} + [xy\ \Omega_X - (1 + x^2)\,\Omega_Y + y\ \Omega_Z\ ]\ , \tag{2a}$$

$$v_y = \left\{ y \frac{V_Z}{Z} - \frac{V_Y}{Z} \right\} + [(1 + y^2)\,\Omega_X - xy\ \Omega_Y - x\ \Omega_Z\ ]\ . \tag{2b}$$

These equations define an instantaneous image flow field, assigning a unique 2-D image velocity $\boldsymbol{v}$ to each direction $(x\,,\,y\,)$ in the observer's field of view. For our formulation, we consider only a single surface patch of some object in the field of view.

2.2 Image Flow Equations for Planar Surfaces in Motion

A small but finite surface patch may be locally approximated by a quadric surface described by six parameters: its distance along the line of sight Z_0 (assumed to be greater than zero throughout), its two slopes T_X, T_Y and three curvatures. If this surface patch is described in our viewer-centered spatial coordinate system by $Z = f(X, Y)$, then using (1), its local representation $Z = f(x, y)$ can be obtained as a second-order polynomial in terms of image coordinates [1]. Using this representation of the surface and performing a kinematic analysis of the image velocity equations (2) in a small neighborhood around the line of sight, we can derive a set of twelve non-linear, algebraic equations relating the motion and structure of the surface to a set of "observables" or

"deformation parameters". In these equations, the distance Z_0 between the surface and the camera along the line of sight always appears in ratio with the translational velocity V and therefore is not recoverable (from a monocular flow field). The deformation parameters are linear combinations of partial derivatives (up to second order) of the image velocity field evaluated at the center of the field of view. They describe the geometrical distortion of the image in a small neighborhood around the line of sight. For planar surfaces represented in the form $Z = Z_0 + T_X X + T_Y Y$, since the curvatures vanish, we get the following eight independent equations and four consrtaints:

$$O_1 = -V_x - \Omega_Y , \tag{3a}$$

$$O_2 = -V_y + \Omega_X , \tag{3b}$$

$$O_3 = V_z + V_x T_X , \tag{3c}$$

$$O_4 = V_z + V_y T_Y , \tag{3d}$$

$$O_5 = \frac{1}{2} (V_y T_X + V_x T_Y) , \tag{3e}$$

$$O_6 = -\Omega_Z + \frac{1}{2} (V_y T_X - V_x T_Y) , \tag{3f}$$

$$O_7 = -2 (\Omega_Y + V_z T_X) , \tag{3g}$$

$$O_8 = \Omega_X - V_z T_Y , \tag{3h}$$

and

$$O_9 = \frac{1}{2} O_7 , \quad O_{12} = \frac{1}{4} O_7 , \tag{4a,b}$$

$$O_{10} = 2 O_8 , \quad O_{11} = -\frac{1}{2} O_8 . \tag{4c,d}$$

where

$$V_x = \frac{V_X}{Z_0}, \quad V_y = \frac{V_Y}{Z_0}, \quad V_z = \frac{V_Z}{Z_0} \text{ for } Z_0 > 0, \tag{5}$$

and

$$O_1 = v_x, \quad O_2 = v_y, \quad O_3 = \frac{\partial v_x}{\partial x}, \quad O_4 = \frac{\partial v_y}{\partial y}, \tag{6a-d}$$

$$O_5 = \frac{1}{2}\left(\frac{\partial v_x}{\partial y} + \frac{\partial v_y}{\partial x}\right), \quad O_6 = \frac{1}{2}\left(\frac{\partial v_y}{\partial x} - \frac{\partial v_x}{\partial y}\right), \tag{6e,f}$$

$$O_7 = \frac{\partial^2 v_x}{\partial x^2}, \quad O_8 = \frac{\partial^2 v_x}{\partial x\, \partial y}, \quad O_9 = \frac{\partial^2 v_y}{\partial x\, \partial y}, \quad O_{10} = \frac{\partial^2 v_y}{\partial y^2} \tag{6g-j}$$

$$O_{11} = \frac{1}{2}\left(\frac{\partial^2 v_x}{\partial x\, \partial y} - \frac{\partial^2 v_y}{\partial x^2}\right), \quad O_{12} = \frac{1}{2}\left(\frac{\partial^2 v_x}{\partial y^2} - \frac{\partial^2 v_y}{\partial x\, \partial y}\right). \tag{6k,l}$$

The quantities O_1 through O_{12} are the image deformation parameters computed at the origin of the image plane. These deformation parameters can be computed if the image velocities at four points (no three of them collinear) on the image plane are known (by fitting a second-order polynomial in image coordinates to the velocity field; see the next section.). Also, two methods of extracting these deformation parameters using contours from successive image frames have been described by Waxman and Wohn [2].

The image flow equations (3) form a set of eight coupled, non-linear algebraic equations among eight unknowns. The method used in [1] to solve these eight equations involved numerically computing a transform angle which aligned one of the image axes with the direction of zero slope at the point on the surface intersected by the line of sight. In Section 5 we describe a new approach to solve these eight equations which requires only the solution of a cubic equation.

3. DUALITY OF PLANAR SURFACE SOLUTIONS

The fact that the image flow equations (3) are non-linear implies the possibility of multiple solutions corresponding to more than one interpretation of the scene. In fact, it was shown in [1] that for any non-zero value of V_z satisfying equations (3), there are two solutions $(V/Z_0, \Omega, T_X, T_Y)$, $(\hat{V}/Z_0, \hat{\Omega}, \hat{T}_X, \hat{T}_Y)$ which satisfy the following duality relationship:

$$\hat{T}_X = -V_x \,/\, V_z \,, \tag{7a}$$

$$\hat{T}_Y = -V_y \,/\, V_z \,, \tag{7b}$$

$$\hat{V}_x = -T_X V_z \,, \tag{7c}$$

$$\hat{V}_y = -T_Y V_z \,, \tag{7d}$$

$$\hat{V}_z \equiv V_z \,, \tag{7e}$$

$$\hat{\Omega}_X = \Omega_X - V_y - V_z T_Y \,, \tag{7f}$$

$$\hat{\Omega}_Y = \Omega_Y + V_x + V_z T_X \,, \tag{7g}$$

$$\hat{\Omega}_Z = \Omega_Z + V_x T_Y - V_y T_X \,. \tag{7h}$$

Notice how the slopes T_X, T_Y and the components of translation parallel to the image plane V_x, V_y play interchangeable roles in the two solutions. There are two exceptions to this duality. The first is when $V_z = 0$ (i.e. the velocity component along the line of sight is zero) and the second is when the translational velocity through space is parallel to the surface normal (i.e. $V_x / V_z = -T_X$ and $V_y / V_z = -T_Y$) in which case equations (7) degenerate to identities. Many numerical examples in [1] had indicated that there was only one value of V_z which satisfied equations (3), thereby suggesting that there are at most two solu-

tions to equations (3). A formal proof of this is given in Section 4. We illustrate the nature of the dual solutions below.

3.1 Illustration of Dual Solutions

In the recovery of surface structure and 3-D motion from image flow, it has been shown that it is sufficient to describe an image flow as a locally second-order flow field [1,2]. This has implications with regard to the surfaces which generate the flow itself. For example, consider a planar surface patch

$$Z = Z_0 + T_X\, X + T_Y\, Y \quad \text{for } Z_0 > 0\,. \tag{8}$$

Using relations (1), this may be expressed in terms of image coordinates as $Z = Z_0(1-T_X x - T_Y y)^{-1}$. Substitution of this into the image velocity equations (3) yields the following expressions which are in the form of a second-order polynomial in the image coordinates:

$$v_x = (xV_z - V_x)(1-T_X x - T_Y y) + \left[xy\,\Omega_X - (1+x^2)\,\Omega_Y + y\,\Omega_Z \right] \tag{9a}$$

$$v_y = (yV_z - V_y)(1-T_X x - T_Y y) + \left[(1+y^2)\,\Omega_X - xy\,\Omega_Y - x\,\Omega_Z \right] \tag{9b}$$

For planar surfaces, such second-order flows are *globally valid* (for quadric surfaces the flow can be *locally approximated* as second-order). The coefficients of this second-order flow then determine the slopes and (scaled) space motion of the planar surface.

Since the above two equations are globally valid, image velocities at four points (no three of them collinear) or more on the plane allow a solution to be

obtained. Of course normal flow along contours (or edge fragments) may be used as well [2]. We can graphically illustrate this duality of solutions by reexpressing the slopes in terms of angles:

$$T_X = \tan\theta \quad \text{and} \quad T_Y = \tan\phi \quad \text{for} \ -\frac{\pi}{2} \le \theta, \phi < \frac{\pi}{2}, \tag{10}$$

and then searching the θ–ϕ space for solutions. Substitution of values for T_X, T_Y renders equations (9) linear in the unknown motion parameters. Therefore, if image velocities at more than four points are known (and the data is noisy), a linear least-square error minimization technique can be used to solve for the corresponding motion parameters. A typical plot of the least-square error in the θ–ϕ space is shown in Figure 2. The actual error values have been thresholded and inverted so that peaks in the figure represent error minima. Locations of peaks representing zero error (for noise-free data) give the solutions for θ and ϕ. In the figure we see that there are two such peaks corresponding to two dual solutions. In Figure 3 we illustrate how the solution for structure (and consequently motion) becomes unique as the velocity component V_z along the line of sight approaches zero. As $V_z \rightarrow 0$, one of the two peaks corresponding to a dual solution (from Figure 2) moves towards the boundary of the θ–ϕ space and finally "disappears", resulting in a unique interpretation. This is consistent with the duality relations (6a,b) in which $\hat{T}_X$ and $\hat{T}_Y$ approach infinity. In Figure 4 we illustrate the behavior of the dual solutions as the direction of the translational velocity V approaches the direction normal to the planar surface. In this case, the peaks (from Figure 2) gradually move towards each other and finally merge into one giving again a unique interpretation.

The above method can, in principle, be used to solve the image flow problem for planar surfaces. We need to search the θ–ϕ space completely only once at the begining of the sequence; this search can be done efficiently by first carrying out the search at coarse intervals and then at finer intervals. For subsequent images, we can evolve the initial solution to the next time instant using the expressions derived in the next section, and search a small neighborhood around this new predicted solution. When the image velocity data is noisy (e.g. as much as 20% perturbations), we have found it very useful to first filter the noise by fitting second-order polynomials to the flow field by least-square error minimization over all the points. The search over θ–ϕ space is then based on this second-order flow field.

3.2 Extraction of Deformation Parameters from Points

Expanding equations (9) and expressing them as polynomials in image coordinates, we find

$$v_x(x,y) = a + bx + cy + dx^2 + d''xy \quad \text{and} \tag{11a}$$

$$v_y(x,y) = a' + b'y + c'y + d''y^2 + dxy \tag{11b}$$

where

$$a = -V_x - \Omega_Y, \qquad a' = -V_y + \Omega_X, \tag{12a,b}$$

$$b = V_z + V_x T_X, \qquad b' = V_z + V_y T_Y, \tag{12c,d}$$

$$c = \Omega_Z + V_x T_Y, \qquad c' = -\Omega_Z + V_y T_X, \tag{12e,f}$$

$$d = -\Omega_Y - V_z T_X, \qquad d'' = -\Omega_X - V_z T_Y. \tag{12g,h}$$

The eight coefficients $a, b, c, d, a', b', c', d'$ can be found if v_x, v_y are known at four points (no three points collinear) or more, by solving the system of linear equations (11). If these velocities are known at more than four points (for noisy data), the coefficients are solved by a linear least-square error minimization method. By inspection of equations (3) and (12), we see that the deformation parameters $O_1 - O_8$ can be obtained from the eight coefficients:

$$O_1 = a \ , \ O_2 = a' \ , \ O_3 = b \ , \ O_4 = b' \ , \tag{13a-d}$$

$$O_5 = \frac{1}{2}(c + c') \ , \ O_6 = \frac{1}{2}(c' - c) \ , \ O_7 = 2d \ , \ O_8 = d'. \tag{13e-h}$$

From these deformation parameters, we can immediately obtain the solution for the 3-D structure and motion parameters of the planar surface in closed form by the methods developed in the following sections.

4. UNIQUENESS OF INTERPRETATION

The image deformation parameters $O_1 - O_8$ introduced in Section 2 may be computed for a planar surface in motion from a pair of successive image frames either by tracking four or more points or by observing an evolving contour on the surface [2]. Utilizing more than two frames will allow a more accurate determination of these parameters. These image deformation parameters completely describe the instantaneous image flow field. But an instantaneous flow field in itself is inherently ambiguous as it has two interpretations for the orientation and motion of the planar surface. This ambiguity in interpretation is manifest in the duality of solutions to equations (3) as discussed in Section 3.

In this section, we show that the interpretation for structure and motion of planar surfaces is uniquely determined in two cases. The first case is when two successive flow fields (or three successive image frames) with one planar surface are given, and the second is when one flow field (or two successive image frames) with two planar surface patches moving as a rigid body is given. Notice that from three consecutive image frames we can extract two sets of image deformation parameters, one set from each pair of consecutive frames. Each of these deformation parameter sets describes the instantaneous velocity field at the mean of the two time instants (in the limit as $\delta t \rightarrow 0$) of the image frame pair from which it is extracted. We will see below that, although solving the image flow equations (3) for the first set of deformation parameters may yield two solutions, only one of them will be consistent over time with the second set of deformation

parameters.

4.1 Proof of Uniqueness of Interpretation: One Planar Surface

The scheme of our proof, when two flow fields of a single planar surface are given, is shown in Figure 5. An image flow field F at time t generated by a planar surface in motion has two solutions, say $S = (V_x, V_y, V_z, \Omega_X, \Omega_Y, \Omega_Z, T_X, T_Y)$ and its dual SD which is related to S by relations (7). For these two solutions, assuming that the *motion in space is constant* over a short time, the slope parameters change with time due to rotation and the scaled translational velocity compoments change with time due to the combined effect of translation and rotation (we shall relax this assumption shortly). As a result, after a time δt later, S and SD evolve into two new solutions, say SE and SDE, respectively. (Explicit expressions for SE and SDE are derived in terms of S in the Appendix). The proof of uniqueness of interpretation is that, although S and SD are duals of each other, SE and SDE are not (see Appendix for details). This implies that if F' is the instantaneous flow field at time $t+\delta t$, then only either SE or SDE will be one of its two solutions. If SE is a solution of the image flow field F' then the actual motion and slopes of the planar surface at time t are given by S.

4.2 Resolving Duality for the General Case: One Planar Surface

In general, for the single planar surface case, the space motion may not be constant over the time period $2\delta t$. We can still proceed to resolve the duality as follows. Let I_1, I_2 and I_3 represent three successive image frames of an image sequence taken at very short time intervals δt apart. Then compute the image flow fields (possibly represented as image deformation parameters) F and F' corresponding to the image frame pairs (I_1, I_2) and (I_2, I_3), respectively. Then use the two flow fields F and F' to get dual solution pairs (S, SD) and (S', SD'), respectively. Also, compute the time evolved solutions SE and SDE corresponding to S and SD, respectively, using relations (A12, A13). Now if SE is "closer" to one of S' or SD' than SDE is to either of them, then S is the required solution of F and the solution "closest" to SE among S' and SD' is the required solution of F'.(For reasons that will become apparent in the next section, the determination of "closeness of solutions" may be based entirely on V_z.) Once we have resolved the duality in this manner, in subsequent time steps we need only to repeat the process of selecting the solution which "agrees most" with our predicted solution. Our predicted solutions will not agree exactly with the computed solutions since the time interval δt between image frames may not be small enough, and the motion in space may not be sufficiently constant with time.

Our approach of seeking consistent 3-D interpretations over time may be viewed as a kind of "prediction and verification". We evolve the solutions of flow F forward in time in order to check for the consistent solution among those of F'. This is an application of the principle of "temporal coherence" in the 3-D domain. Our approach may be contrasted with that of Tsai and Huang [3] who select three consecutive image frames I_1, I_2 and I_3, and solve for the parameters of the *backward evolution* $I_2 \rightarrow I_1$ along with the *forward evolution* $I_2 \rightarrow I_3$. Duality is resolved by requiring consistency (equality of the slopes) among the chosen backward solution and its corresponding forward solution.

4.3 Proof of Uniqueness of Interpretation: Two Planar Surfaces

The proof of uniqueness, when a flow field with two planar patches in the scene is given, is quite straightforward. We assume that the two planar surfaces are *stationary in space* with respect to each other (i.e. they move as a rigid body) and neither of them passes through the origin (i.e. $Z_0 \neq 0$). Suppose that solving the flow field for the structure and motion of the two surfaces yields the dual solution pairs $(S^{(1)}, SD^{(1)})$ and $(S^{(2)}, SD^{(2)})$ where

$$S^{(1)} = (V_x^{(1)}, V_y^{(1)}, V_z^{(1)}, \Omega_X{}^{(1)}, \Omega_Y{}^{(1)}, \Omega_Z{}^{(1)}, T_X{}^{(1)}, T_Y{}^{(1)}) \tag{14a}$$

$$S^{(2)} = (V_x^{(2)}, V_y^{(2)}, V_z^{(2)}, \Omega_X{}^{(2)}, \Omega_Y{}^{(2)}, \Omega_Z{}^{(2)}, T_X{}^{(2)}, T_Y{}^{(2)}) \;, \tag{14b}$$

and $SD^{(1)}$ and $SD^{(2)}$ are related to $S^{(1)}$ and $S^{(2)}$ by relations (7). Then we shall show that the solutions corresponding to the actual interpretation for the struc-

ture and motion of the two surfaces, say $S^{(1)}$ and $S^{(2)}$, are uniquely determined.

Suppose that the two surfaces are not parallel (i.e. they have different orientations); then for $S^{(1)}$ and $S^{(2)}$ we have

$$(T_X{}^{(1)}, T_Y{}^{(1)}) \neq (T_X{}^{(2)}, T_Y^{(2)}) . \tag{15a}$$

But for the slopes of $SD^{(1)}$ and $SD^{(2)}$, from relations (5) and (7), we always find that

$$(\hat{T}_X{}^{(1)}, \hat{T}_Y{}^{(1)}) = (\hat{T}_X{}^{(2)}, \hat{T}_Y^{(2)}) \tag{15b}$$

since

$$(-V_x^{(1)}/V_z^{(1)}, -V_y^{(1)}/V_z^{(1)}) = (-V_x^{(2)}/V_z^{(2)}, -V_y^{(2)}/V_z^{(2)}) , \tag{15c}$$

which reflects the rigid body motion of the planar surface pair. Furthermore, $S^{(1)}$ and $S^{(2)}$ have the same rotation parameters, whereas, in general, this is not true with $SD^{(1)}$ and $SD^{(2)}$. Therefore, $SD^{(1)}$ and $SD^{(2)}$ can be ruled out as they are inconsistent.

If the two planar surfaces are in fact parallel but distinct (i.e. $Z_0^{(1)} \neq Z_0^{(2)}$), then $S^{(1)}$ and $S^{(2)}$ still have the same rotation parameters whereas $SD^{(1)}$ and $SD^{(2)}$ do not. Thus, again we can rule out $SD^{(1)}$ and $SD^{(2)}$ as unacceptable.

Therefore, for two (or more) planar surfaces moving as a rigid body (e.g. faces of a polyhedron), a unique 3-D interpretation may be derived from an instantaneous image flow field. Of course, the flow field itself must first be seg-

mented into analytic regions corresponding to individual planar surfaces [5].

Tsai and Huang [6] have arrived at a similar conclusion as a consequence of their general proof of uniqueness for seven points moving rigidly through space. Regarding uniqueness for the specific case of two planar surfaces, our proof is far simpler and more direct.

5. PROOF OF UNIQUENESS FOR V_z

For a planar surface in motion, from two successive image frames, we can extract a set of image deformation parameters which uniquely describe the image flow associated with the image frame pair [2]. Solutions of the image flow equations (3) for these deformation parameters correspond to the possible interpretations associated with the image frame pair. In this section, we show that the relative velocity of approach V_z associated with such an image frame pair is unique. As a consequence of this result, since there is only one pair of dual solutions associated with each possible V_z, there are at most two interpretations associated with two successive image frames.

5.1 Proof

We obtain an equation in V_z by eliminating all other parameters from equations (3) as follows. From equations (3a,b) we have

$$\Omega_Y = -O_1 - V_x \quad \text{and} \quad \Omega_X = O_2 + V_y . \tag{16}$$

Substituting for Ω_X and Ω_Y from above in equations (3g) and (3h) and rearranging terms, we find

$$V_x = V_z\ T_X - A \quad \text{and} \quad V_y = V_z\ T_Y - B\ , \tag{17}$$

where

$$A \equiv O_1 - \frac{1}{2}\, O_7 \quad \text{and} \quad B \equiv O_2 - O_8 . \tag{18}$$

Using the above relations, we eliminate V_x and V_y from (3c-e) to get

$$O_3 = V_z + (V_z\ T_X - A)\ T_X \tag{19a}$$

$$O_4 = V_z + (V_z\ T_Y - B)\ T_Y \tag{19b}$$

$$2O_5 = (V_z\ T_Y - B)\ T_X + (V_z\ T_X - A)\ T_Y\ . \tag{19c}$$

We have here three equations in three unknowns. Equations (19a,b) are quadratic in T_X and T_Y, respectively, with solutions given in terms of V_z as:

$$T_{X+},\ T_{X-} = \frac{A \pm \sqrt{A^2 - 4V_z(V_z - O_3)}}{2V_z} \tag{20a}$$

$$T_{Y+},\ T_{Y-} = \frac{B \pm \sqrt{B^2 - 4V_z(V_z - O_4)}}{2V_z}\ . \tag{20b}$$

Substituting for T_X and T_Y from (20) into (19c) and simplifying, yields

$$4O_5 V_z + AB = \pm\sqrt{[\, A^2 - 4V_z(V_z - O_3)\,]\ \ [\, B^2 - 4V_z(V_z - O_4)\,]}\ . \tag{21}$$

Squaring expression (21) gives

$$V_z\ (\ V_z^3 + C_1\ V_z^2 + C_2\ V_z + C_3\ ) = 0\ , \tag{22}$$

where

$$C_1 = -(O_3 + O_4)\ , \tag{23a}$$

$$C_2 = -(\frac{1}{4}A^2 + \frac{1}{4}B^2 + O_5^2 - O_3\ O_4)\ , \tag{23b}$$

$$C_3 = \frac{1}{4}A^2\ O_4 + \frac{1}{4}B^2\ O_3 - \frac{1}{2}\ O_5\ AB\ . \tag{23c}$$

In equation (22), we disregard the case of $V_z = 0$ since substitution of this into equation (21) leads to an identity not involving V_z (in fact, when $V_z = 0$, equations (3) have a unique solution [1]); therefore equation (22) reduces to a cubic equation in V_z. For convenience, let us express the cubic equation in terms of a

new parameter α:

$$\alpha^3 + C_1 \alpha^2 + C_2 \alpha + C_3 = 0 \tag{24}$$

We can verify that the three roots of equation (24) are

$$\alpha_0, \alpha_+, \alpha_- = V_z \, , \, \frac{1}{2}\left\{ V_x T_X + V_y T_Y + V_z \pm \sqrt{(V_x{}^2 + V_y{}^2 + V_z{}^2)\,(1 + T_X^2 + T_Y^2)} \right\} \tag{25a}$$

by expressing the coefficients C_1, C_2, C_3 in terms of V_x, V_y, V_z, T_X and T_Y. These three roots can be expressed in the following suggestive way:

$$\alpha_0, \alpha_+, \alpha_- = V_z \, , \, \frac{1}{2}\left\{ \boldsymbol{\nu} \cdot \boldsymbol{\lambda} \pm \sqrt{(\boldsymbol{\nu} \cdot \boldsymbol{\nu})\,(\boldsymbol{\lambda} \cdot \boldsymbol{\lambda})} \right\} \tag{25b}$$

where $\boldsymbol{\nu}$ is the scaled translational velocity vector with its Z-component reversed, i.e. $\boldsymbol{\nu} = (V_x, V_y, -V_z)$, and $\boldsymbol{\lambda}$ is a vector normal to the planar surface given by $\boldsymbol{\lambda} = (T_X, T_Y, -1)$.

All three roots (25) are real, but two of them, α_+ and α_-, are extraneous roots introduced by the squaring of equation (21). When these roots are not equal to α_0, back substitution into expressions (20) yields imaginary values for the two slopes (i.e. the radicands are negative). When both radicands are simultaneously zero (i.e. the direction of translational velocity is parallel to the planar surface normal), then relation (21) assigns a unique value to V_z given by $V_z = -(AB)/(4O_5)$ which corresponds to α_0. In general, the root α_0 is the unique solution for V_z.

5.2 Solving for α_0 and the Orientation and Motion Parameters

The fact that the radicands in equations (20) are less than or equal to zero for α_+ and α_- and greater than or equal to zero for α_0 can be used to show that $\alpha_- \leq \alpha_0 \leq \alpha_+$. This relation is useful in selecting α_0 from the three roots of equation (24) without actually substituting them into the radicands of equations (20). For the root α_0 , the radicand in equation (20a) is greater than or equal to zero, i.e. ,

$$A^2 - 4\,\alpha_0\,(\alpha_0 - O_3) \geq 0$$

$$\rightarrow \quad \alpha_0^2 - O_3\,\alpha_0 - \frac{1}{4}A^2 \leq 0$$

$$\rightarrow \quad (\alpha_0 - A_-)\,(\alpha_0 - A_+) \leq 0 \ \left(\text{where } A_+, A_- = (1/2)\,(O_3 \pm \sqrt{O_3^2 + A^2}\,)\right)$$

$$\rightarrow \quad A_- \leq \alpha_0 \leq A_+. \tag{26a}$$

Similarly, for the radicand in (20b) we find

$$B_- \leq \alpha_0 \leq B_+ \ \left(\text{where } B_+, B_- = (1/2)\,(O_4 \pm \sqrt{O_4^2 + B^2}\,)\right). \tag{26b}$$

Hence

$$\max\,(A_-, B_-) \leq \alpha_0 \leq \min\,(A_+, B_+). \tag{26c}$$

Similarly, using the fact that the two radicands are less than or equal to zero for the roots α_+ and α_- , we can derive the following relations:

$$\alpha_+ \geq \max\,(A_+, B_+) \quad \text{and} \quad \alpha_- \leq \min\,(A_-, B_-)\,. \tag{27}$$

Relations (26) and (27) imply that α_0 is the middle root of the cubic equation (24) (i.e. $\alpha_- \leq \alpha_0 \leq \alpha_+$).

Utilizing the closed form solution for the roots of a cubic equation, we find the root α_0 of equation (24) as follows. Let

$$p = \frac{C_2}{3} - \frac{C_1^2}{9} \quad \text{and} \quad q = \frac{C_1^3}{27} - \frac{C_1 C_2}{6} + \frac{C_3}{2}. \tag{28a,b}$$

Then, if $p = 0$,

$$\alpha_0 = \sqrt[3]{-2q} - b/3 ; \tag{29a}$$

if $q = 0$,

$$\alpha_0 = - b/3 ; \tag{29b}$$

otherwise,

$$\alpha_0 = 2\, r\, Cos\left(\frac{\pi + \psi}{3}\right) - \frac{b}{3} \tag{29c}$$

where

$$r = \text{sign}(q)\sqrt{|\, p\, |} \quad \text{and} \quad \psi = Cos^{-1}\left(\frac{q}{r^3}\right). \tag{30a,b}$$

Having solved for $V_z = \alpha_0$, we obtain the remaining parameters as follows. Substitute this value of V_z into equation (21) and determine the sign of the right hand side which satisfies this equation. If this is "+", then the dual solutions for the slopes are $(T_{X+},\ T_{Y+})$ and (T_{X-}, T_{Y-}); if it is "−", the dual solutions for the slopes are (T_{X+}, T_{Y-}) and (T_{X-}, T_{Y+}). At this point we can solve for V_x and V_y using relations (17), and Ω_X and Ω_Y using relations (16). Finally, Ω_Z is found from relation (3f).

6. CONCLUSION

In this paper we have extended the previous work of Waxman & Ullman [1] related to the image flow problem for planar surfaces in motion. We have described methods to disambiguate dual interpretations associated with image flows generated by planar surfaces. We have also obtained closed form solutions to the image flow equations for planar surfaces. Our results suggest a new way of solving the image flow problem for planar surfaces, which we summarize below.

Assuming that the image deformation parameters (which can be obtained by either tracking points or contours on the image plane) at two time instants t and $t+dt$ are known, the key steps of this new method for the single surface case are as follows:

a) Initially, at time t check if the velocity of approach along the line of sight is zero by noting if the following condition is satisfied:

$$O_5 = \frac{1}{2}\left\{ \frac{B}{A} O_3 + \frac{A}{B} O_4 \right\} , \tag{31}$$

where A and B are as in equations (18). If the above condition is satisfied (or nearly so in the presence of noise), then the image flow equations (3) have a unique solution which can be easily computed directly from the deformation parameters [1]. If the condition is not satisfied, then proceed with the following steps.

b) Compute $V_z = \alpha_0$ from the deformation parameters and then obtain the

remaining unknowns as described in Section 5. At this point, if there are two distinct (dual) solutions, proceed to the next step; otherwise, the unique solution obtained gives the actual motion and orientation of the planar surface.

c) Repeat steps (a) and (b) using the the image deformation parameters at time $t+dt$, and using the method discussed in Section 4 resolve the duality to obtain a unique solution.

If there are two (or more) planar surfaces moving as a rigid body in the scene, then in step (b), resolve the ambiguity of interpretation by the method described in Section 4.3.

APPENDIX:

EVOLUTION OF PLANAR SURFACE SOLUTIONS

At time instant t, let a planar surface in motion be described by

$$Z = Z_0 + T_X X + T_Y Y \tag{A1}$$

in the coordinate system shown in Figure 1, where Z_0 is the Z intercept of the plane and T_X, T_Y are the X and Y slopes respectively. Also, let V and Ω be the relative translational and rotational velocities in space of an observer with respect to the planar surface. This *relative motion* in space is *assumed constant* over short time intervals (over three image frames). We represent the relative motion of the observer and the structure of the plane at time t in matrix form as:

$$S = \begin{bmatrix} V_x & V_y & V_z \\ \Omega_X & \Omega_Y & \Omega_Z \\ T_X & T_Y & Z_0 \end{bmatrix} . \tag{A2}$$

In this matrix, the first row represents the translational velocity components scaled by distance Z_0, the second row the rotational velocity components and the third row the slopes of the plane and the distance scale factor. The motion and structure parameters, represented by S above, change with time due to the relative motion between the plane and the observer's reference frame. In the remaining part of this section we derive expressions for these parameters after a small time interval dt has elapsed.

To compute the change in the structure parameters during the time interval dt, we first take the time derivative on either side of equation (A1) to get

$$\frac{dZ}{dt} = \frac{dZ_0}{dt} + T_X \frac{dX}{dt} + X \frac{dT_X}{dt} + T_Y \frac{dY}{dt} + Y \frac{dT_Y}{dt} . \tag{A3}$$

The time derivatives of (X, Y, Z) in the above expression are given by the three components of the vector $-(V + \Omega \times R)$ respectively which describes the relative motion of a point $R = (X, Y, Z)$ with respect to the reference frame. Substituting these components for the derivatives, and $Z_0 + T_X X + T_Y Y$ for Z and rearranging terms, we get

$$\left\{ \frac{dZ_0}{dt} - Z_0 ((\Omega_Y + V_X / Z_0) T_X - (\Omega_X - V_Y / Z_0) T_Y - V_Z / Z_0) \right\} +$$

$$\left\{ \frac{dT_X}{dt} - (T_X (\Omega_Y T_X - \Omega_X T_Y) + (\Omega_Y + \Omega_Z T_Y)) \right\} X +$$

$$\left\{ \frac{dT_Y}{dt} - (T_Y (\Omega_Y T_X - \Omega_X T_Y) - (\Omega_X + \Omega_Z T_X)) \right\} Y = 0 .$$

In the above expression, since X, Y are independent parameters of points on the plane in motion, we can equate each of the three terms above to zero separately to get the exact differentials for the slopes and distance as

$$dZ_0 = Z_0 \left[(\Omega_Y + V_z) T_X - (\Omega_X - V_y) T_Y - V_z \right] dt , \tag{A4a}$$

$$dT_X = \left[T_X (\Omega_Y T_X - \Omega_X T_Y) + (\Omega_Y + \Omega_Z T_Y) \right] dt , \tag{A4b}$$

$$dT_Y = \left[T_Y (\Omega_Y T_X - \Omega_X T_Y) - (\Omega_X + \Omega_Z T_X) \right] dt . \tag{A4c}$$

Using the above relations, we can compute the new structure parameters at time $t + dt$ as

$$T'_X = T_X + dT_X \ , \ \ T'_Y = T_Y + dT_Y \ \text{ and } \ Z'_0 = Z_0 + dZ_0 \ . \tag{A5a-c}$$

The new translational velocity V' at time $t+dt$ is found (in the absence of accelerations) from

$$V' = V + V \times \Omega \ dt \ . \tag{A6}$$

Dividing V' by Z'_0 and simplifying, we get the new scaled velocity components

$$V'_x = V_x + (V_y \Omega_Z - V_z \Omega_Y - V_x \ s) \ dt + O(dt^2) \ , \tag{A7a}$$

$$V'_y = V_y + (V_z \Omega_X - V_x \Omega_Z - V_y \ s) \ dt + O(dt^2) \ , \tag{A7b}$$

$$V'_z = V_z + (V_x \Omega_Y - V_y \Omega_X - V_z \ s) \ dt + O(dt^2) \ , \tag{A7c}$$

where

$$s \equiv (\Omega_Y + V_x) T_X - (\Omega_X - V_y) T_Y - V_z \ . \tag{A8}$$

The rotational velocity remains unchanged since

$$\Omega' = \Omega + \Omega \times \Omega \ dt \ = \ \Omega \ . \tag{A10}$$

Summarizing the above results, we have that, if the structure of a planar surface and the instantaneous motion of an observer relative to the planar surface at time t is S given by (A2), and at time $t+dt$ is SE given by

$$SE = \begin{bmatrix} V'_x & V'_y & V'_z \\ \Omega'_X & \Omega'_Y & \Omega'_Z \\ T'_X & T'_Y & Z'_0 \end{bmatrix} , \tag{A11}$$

then S and SE are related as below.

$$\begin{bmatrix} V'_x \\ V'_y \\ V'_z \end{bmatrix} = \begin{bmatrix} V_x \\ V_y \\ V_z \end{bmatrix} + \begin{bmatrix} -s & \Omega_Z & -\Omega_Y \\ -\Omega_Z & -s & \Omega_X \\ \Omega_Y & -\Omega_X & -s \end{bmatrix} \begin{bmatrix} V_x \\ V_y \\ V_z \end{bmatrix} dt \ , \tag{A12a}$$

$$(\Omega'_X , \Omega'_Y , \Omega'_Z) = (\Omega_X , \Omega_Y , \Omega_Z) \quad \text{and} \tag{A12b}$$

$$\begin{bmatrix} T'_X \\ T'_Y \\ Z'_0 \end{bmatrix} = \begin{bmatrix} T_X \\ T_Y \\ Z_0 \end{bmatrix} + \begin{bmatrix} \Omega_Y T_X - \Omega_X T_Y & \Omega_Z & \Omega_Y \\ -\Omega_Z & \Omega_Y T_X - \Omega_X T_Y & -\Omega_X \\ Z_0(\Omega_Y + V_z) & -Z_0(\Omega_X - V_y) & -Z_0 V_z \end{bmatrix} \begin{bmatrix} T_X \\ T_Y \\ 1 \end{bmatrix} dt. \tag{A12c}$$

Now we refer the reader to Figure 5 for the scheme of our proof of uniqueness. From our discussion in Section 3, the instantaneous image velocity field corresponding to S has another solution SD which is the dual of S given by

$$SD = \begin{bmatrix} -T_X V_z & -T_Y V_z & V_z \\ \Omega_X - V_y - V_z T_Y & \Omega_Y + V_z + V_z T_X & \Omega_Z + V_z T_Y - V_y T_X \\ -V_z / V_z & -V_y / V_z & Z_0 \end{bmatrix} . \tag{A13}$$

We have expressed SD and SE in terms of S. Let SDE denote the new solution obtained by evolving SD in time to $t+dt$. SDE can be obtained by substituting the elements of SD for the corresponding elements of S in expression (A12) for SE. The proof of uniqueness of interpretation is that, at time t, although S and SD are the two dual interpretations of a planar surface in motion, at time $t+dt$, their time evolved solutions, SE and SDE respectively, are not duals. A simple way to verify that SE and SDE are not duals is to note that their Z-components of translational velocity are not the same (for dual solutions, this should be the same.). It can be shown easily that the values of this velocity component for SE and SDE are related by

$$V_{z\,(SDE)} = V_{z\,(SE)} + (V_z^2 - V_z^2 T_X^2 + V_y^2 - V_z^2 T_Y^2) \, dt \tag{A14}$$

The two velocity components are the same (i.e. the term with dt above vanishes) when the direction of translational velocity is parallel to the plane's normal, in

which case the interpretation is unique according to our discussion in Section 3.

References

[1] A.M. Waxman and S. Ullman, "Surface Structure and 3-D Motion From Image Flow: A Kinematic Analysis", CAR-TR-24, Center for Automation Research, University of Maryland, October 1983.

[2] A.M. Waxman and K. Wohn, "Contour Evolution, Neighborhood Deformation and Global Image Flow: Planar Surfaces in Motion", CAR-TR-58, Center for Automation Research, University of Maryland, April 1984.

[3] R.Y. Tsai and T.S. Huang, "Estimating Three-Dimensional Motion Parameters of a Rigid Planar Patch", Technical Report R-922, Coordinated Science Laboratory, University of Illinois, Urbana, November 1981.

[4] B.F. Buxton, H. Buxton, D.W. Murray and N.S. Williams, "3D Solutions to the Aperture Problem", ECAI '84.

[5] K. Wohn and A.M. Waxman, "The Analytic Structure of Image Flows: Deformation and Segmentation", Center for Automation Research, Technical Report in preparation, University of Maryland, 1985.

[6] R.Y. Tsai, T.S. Huang, "Uniqueness and Estimation of Three-Dimensional Motion Parameters of Rigid Objects with Curved Surfaces", Technical Report R-921, Coordinated Science Laboratory, University of Illinois, Urbana, October 1981.

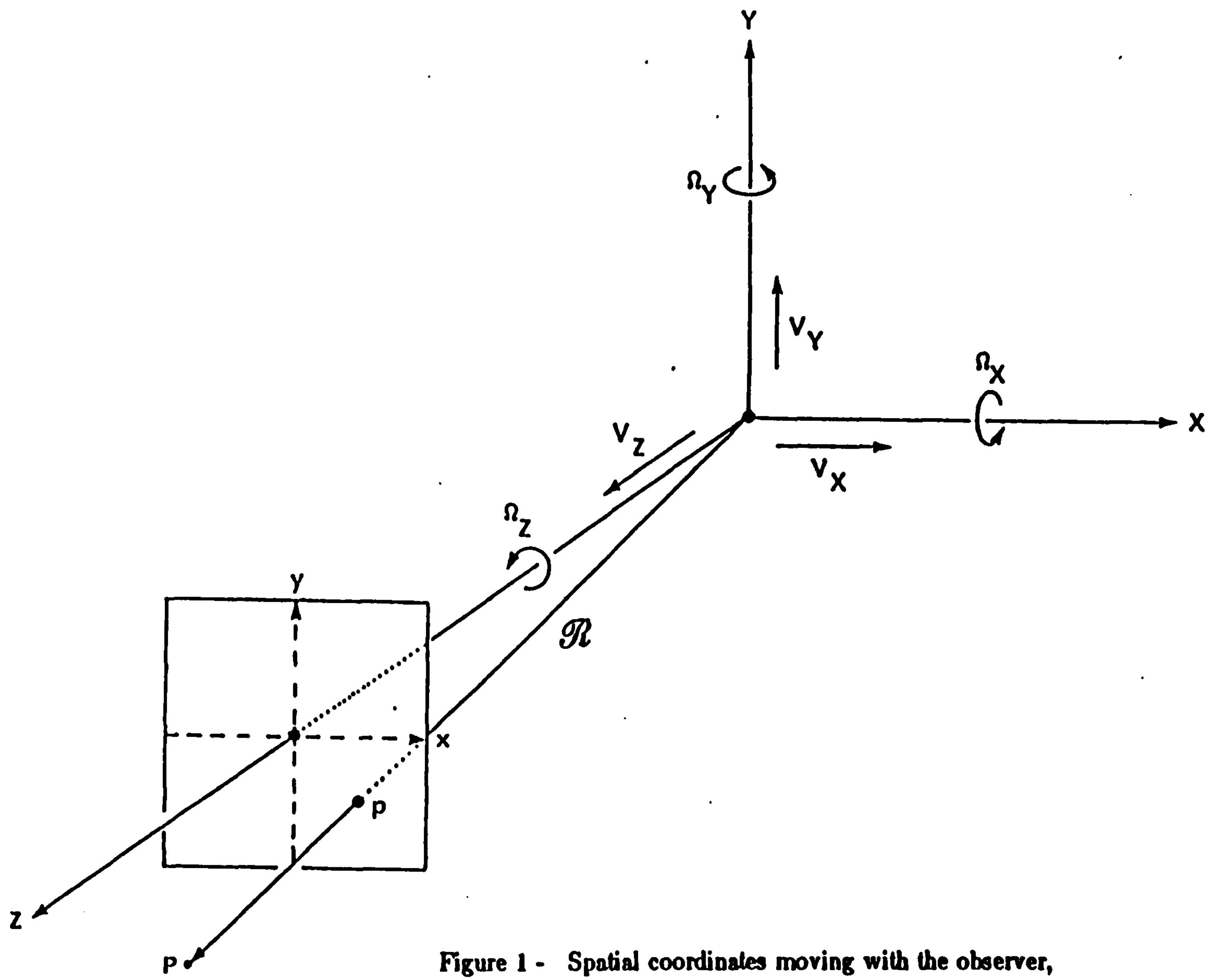

Figure 1 - Spatial coordinates moving with the observer, and image coordinate system.

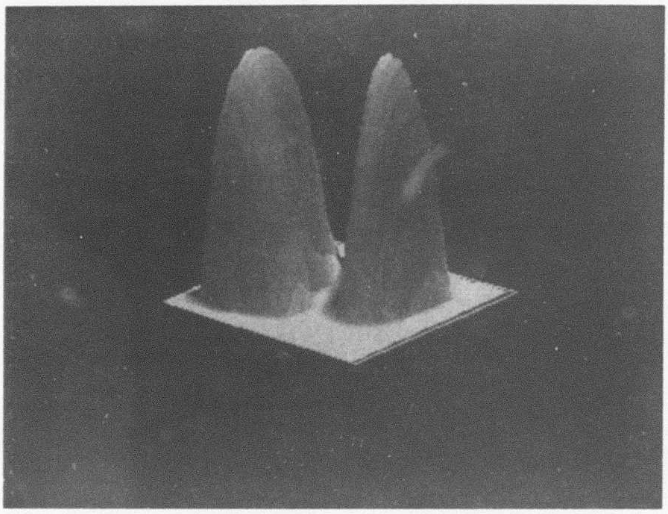

Figure 2. Illustration of least square error in the $\theta - \phi$ space. The two peaks in the figure represent error minima and their locations give the two dual solutions. Here, the scaled velocity component along the line of sight is $V_z = 0.4$ and the angle between V and the surface normal is $\beta = 93^o$.

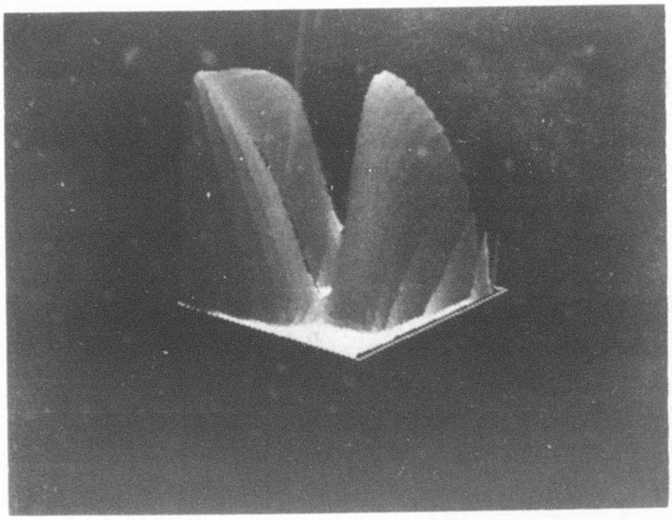

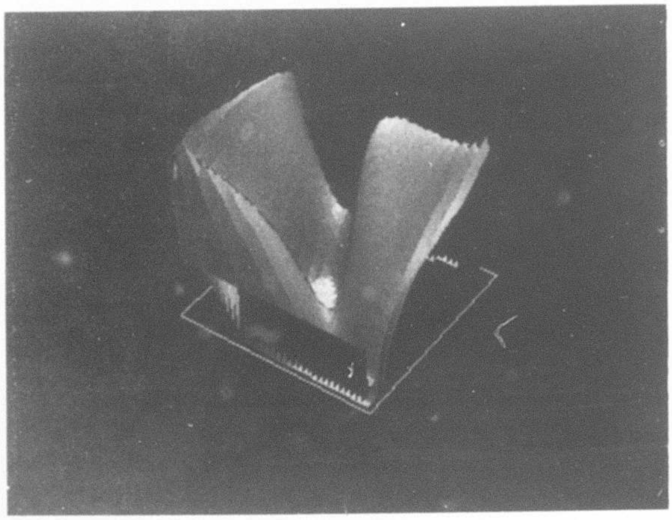

(a) (b)

Figure 3. Behavior of dual solutions as the velocity component along the line of sight approaches zero. Begining from Figure 2, we see that, as $V_z \rightarrow 0$, one of the peaks moves towards the edge of the $\theta - \phi$ space and eventually "disappears" resulting in a unique solution. (a) $V_z = 0.1$. (b) $V_z = 0.01$.

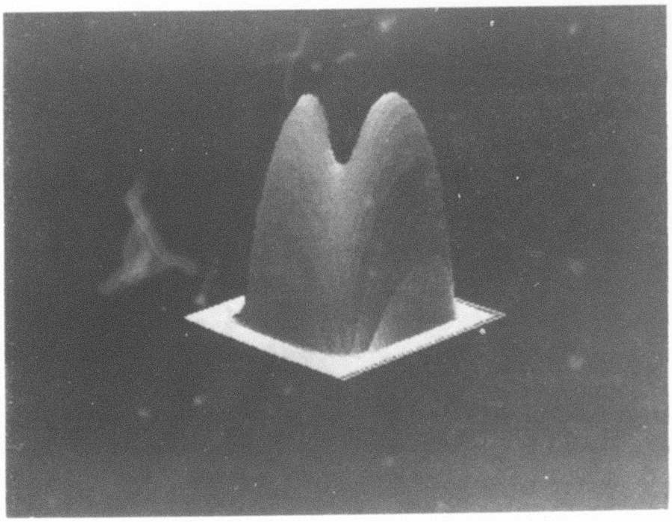

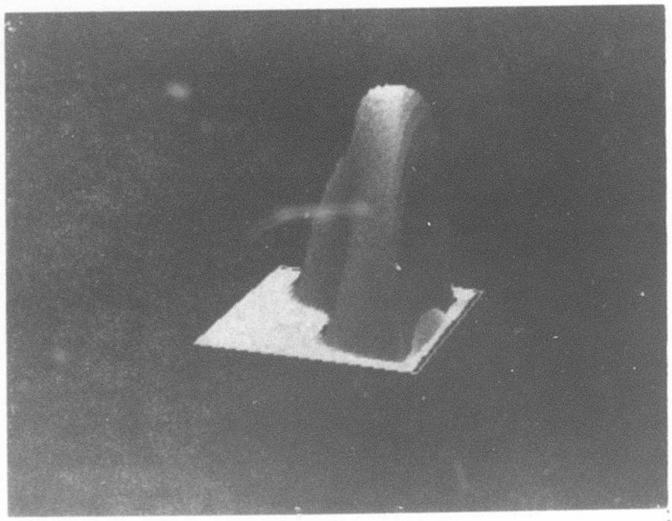

(a) (b)

Figure 4. Behavior of dual solutions as the direction of V approaches that of the surface normal. Begining from Figure 2, we see that, as $\beta \rightarrow 0$, one of the peaks moves towards the other and eventually merges with it resulting in a unique solution. (a) $\beta = 67^o$. (b) $\beta = 0^o$.

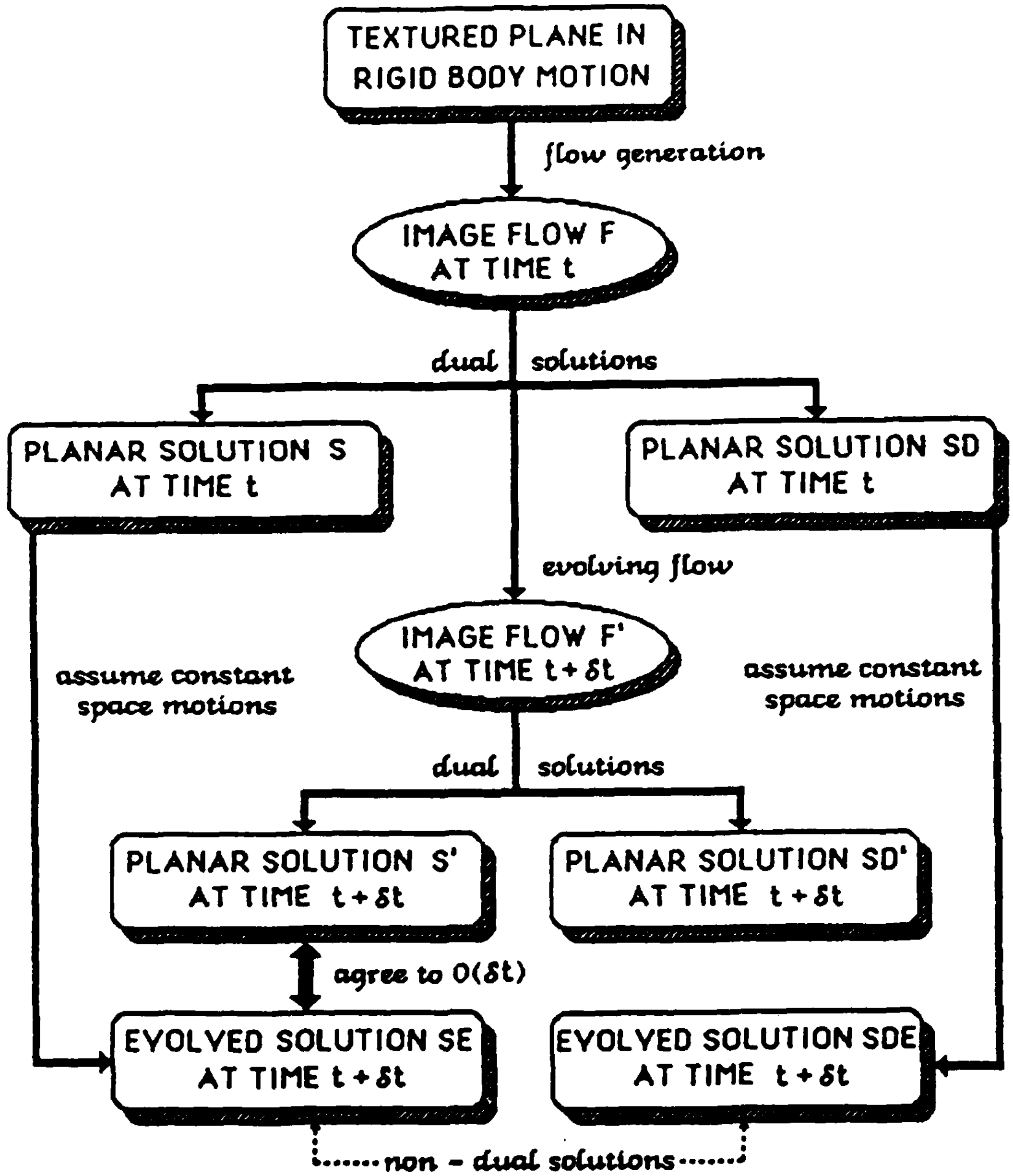

Figure 5. The uniqueness of the 3-D interpretation for planar surfaces in motion stems from coherence over time.

UNCLASSIFIED

SECURITY CLASSIFICATION OF THIS PAGE

AD-A158 705

REPORT DOCUMENTATION PAGE

1a. REPORT SECURITY CLASSIFICATION: UNCLASSIFIED

1b. RESTRICTIVE MARKINGS: N/A

2a. SECURITY CLASSIFICATION AUTHORITY: N/A

2b. DECLASSIFICATION/DOWNGRADING SCHEDULE: N/A

3. DISTRIBUTION/AVAILABILITY OF REPORT: Approved for public release; distribution unlimited

4. PERFORMING ORGANIZATION REPORT NUMBER(S): CAR-TR-114, CS-TR-1485

5. MONITORING ORGANIZATION REPORT NUMBER(S): N/A

6a. NAME OF PERFORMING ORGANIZATION: University of Maryland

6b. OFFICE SYMBOL (If applicable): N/A

7a. NAME OF MONITORING ORGANIZATION: U.S.Army Night Vision and Electro-Optics Laboratory

6c. ADDRESS (City, State and ZIP Code): Center for Automation Research, College Park, MD 20742

7b. ADDRESS (City, State and ZIP Code): Fort Belvoir, VA 22060

8a. NAME OF FUNDING/SPONSORING ORGANIZATION: DARPA

8b. OFFICE SYMBOL (If applicable): IPTO

9. PROCUREMENT INSTRUMENT IDENTIFICATION NUMBER: DAAK70-83-K-0018

8c. ADDRESS (City, State and ZIP Code): 1400 Wilson Blvd. Arlington, VA 22209

10. SOURCE OF FUNDING NOS.

PROGRAM ELEMENT NO.	PROJECT NO.	TASK NO.	WORK UNIT NO.

11. TITLE (Include Security Classification): ON THE UNIQUENESS OF IMAGE FLOW SOLUTIONS FOR PLANAR SURFACES IN MOTION

12. PERSONAL AUTHOR(S): Muralidhara Subbarao and Allen M. Waxman

13a. TYPE OF REPORT: Technical

13b. TIME COVERED: FROM N/A TO

14. DATE OF REPORT (Yr., Mo., Day): April 1985

15. PAGE COUNT:

16. SUPPLEMENTARY NOTATION:

17. COSATI CODES

FIELD	GROUP	SUB. GR.

18. SUBJECT TERMS (Continue on reverse if necessary and identify by block number)

19. ABSTRACT (Continue on reverse if necessary and identify by block number)

Two important results relating to the uniqueness of image flow solutions for planar surfaces in motion are presented here. These results relate to the formulation of the image flow problem by Waxman and Ullman [1], which is based on a kinematic analysis of the image flow field. The first result concerns resolving the duality of interpretations that are generally associated with the instantaneous image flow of an evolving image sequence. It is shown that the interpretation for orientation and motion of planar surfaces is unique when either two successive image flows of one planar surface patch are given or one image flow of two planar patches moving as a rigid body is given. We have proved this by deriving explicit expressions for the evolving solution of an image flow sequence with time. These expressions can be used to resolve this ambiguity of interpretation in practical problems. The second result is the proof of uniqueness for the velocity of approach which satisfies the image flow equations for planar surfaces derived in [1]. In addition, it is shown that this velocity can be computed as the middle root of a cubic equation. These two results

(continued on back)

20. DISTRIBUTION/AVAILABILITY OF ABSTRACT: UNCLASSIFIED/UNLIMITED ☒ SAME AS RPT. ☐ DTIC USERS ☐

21. ABSTRACT SECURITY CLASSIFICATION: UNCLASSIFIED

22a. NAME OF RESPONSIBLE INDIVIDUAL:

22b. TELEPHONE NUMBER (Include Area Code):

22c. OFFICE SYMBOL:

DD FORM 1473, 83 APR — EDITION OF 1 JAN 73 IS OBSOLETE.

UNCLASSIFIED

SECURITY CLASSIFICATION OF THIS PAGE

19. Abstract (continued)

together suggest a new method for solving the image flow problem for planar surfaces in motion.